



^aDepartment of Neurology, Graduate School of Medicine, Osaka University, Osaka, Japan;

^bDepartment of Pathology, Graduate School of Medicine, Osaka University, Osaka, Japan;

^cNeuroregeneration and Stem Cell Programs, Institute for Cell Engineering, Johns Hopkins University School of Medicine, Baltimore, Maryland, USA;

^dDivision of Stem Cell Research, Department of Biomedical Research and Innovation, Institute for Clinical Research, National Hospital Organization Osaka National Hospital, Osaka, Japan;

^eLaboratory Animal Research Department, Biomedical Research Laboratory, Central Institute for Experimental Animals, Kanagawa, Japan;

^fGraduate School of Frontier Biosciences, Osaka University, Osaka, Japan;

^gDepartment of Human Genetics, National Center for Child Health and Development, Tokyo, Japan;

^hDivision of Regenerative Medicine, Department of Biomedical Research and Innovation, Institute for Clinical Research, National Hospital Organization Osaka National Hospital, Osaka, Japan;

ⁱDepartment of Neurosurgery, National Hospital Organization Osaka National Hospital, Osaka, Japan;

^jDepartment of Physiology, Keio University School of Medicine, Shinjuku, Tokyo, Japan

*Co-first authors.

†Co-senior authors.

*Co-first authors.

†Co-senior authors.

Correspondence: Yasuyoshi Kimura, M.D., Ph.D. Neuroregeneration and Stem Cell Programs, Institute for Cell Engineering, Johns Hopkins University School of Medicine, 733 North Broadway, Edward D. Miller Research Building (MRB), 731, Baltimore, Maryland 21205, USA. Telephone: 1-410-614-3359; e-mail: ykimura4@jhmi.edu; or Hideki Mochizuki, M.D., Ph.D., Department of Neurology, Osaka University Graduate School of Medicine, Yamadaoka 2-2, Suita, Osaka 565-0871, Japan. Telephone: 81-6-6879-3720; e-mail: hmochizuki@neuro.med.osaka-u.ac.jp

Received February 25, 2018; accepted for publication February 20, 2019; first published March 19, 2019.

<http://dx.doi.org/10.1002/sctm.18-0039>

This is an open access article under the terms of the Creative Commons Attribution-NonCommercial-NoDerivs License, which permits use and distribution in any medium, provided the original work is properly cited, the use is non-commercial and no modifications or adaptations are made.

Human Genomic Safe Harbors and the Suicide Gene-Based Safeguard System for iPSC-Based Cell Therapy

YASUYOSHI KIMURA^{1b},^{a,b,c,*} TOMOKO SHOFUDA,^{d,*} YUICHIRO HIGUCHI,^e IPPEI NAGAMORI,^b MASAOKI ODA,^{b,f} MASAYUKI NAKAMORI,^a MASAFUMI ONODERA,^g DAISUKE KANEMATSU,^h ATSUYO YAMAMOTO,^d ASAKO KATSUMA,^h HIROSHI SUEMIZU,^e TORU NAKANO,^{b,f} YONEHIRO KANEMURA,^{h,i,j,†} HIDEKI MOCHIZUKI^{a,†}

Key Words. Induced pluripotent stem cells • Genomic safe harbor • Gene editing • Teratoma • Suicide gene • Regenerative medicine

ABSTRACT

The use of human induced pluripotent stem cells (hiPSCs) and recent advances in cell engineering have opened new prospects for cell-based therapy. However, there are concerns that must be addressed prior to their broad clinical applications and a major concern is tumorigenicity. Suicide gene approaches could eliminate wayward tumor-initiating cells even after cell transplantation, but their efficacy remains controversial. Another concern is the safety of genome editing. Our knowledge of human genomic safe harbors (GSHs) is still insufficient, making it difficult to predict the influence of gene integration on nearby genes. Here, we showed the topological architecture of human GSH candidates, *AAVS1*, *CCR5*, *human ROSA26*, and an extragenic GSH locus on chromosome 1 (Chr1-eGSH). Chr1-eGSH permitted robust transgene expression, but a 2 Mb-distant gene within the same topologically associated domain showed aberrant expression. Although knockin iPSCs carrying the suicide gene, *herpes simplex virus thymidine kinase (HSV-TK)*, were sufficiently sensitive to ganciclovir in vitro, the resulting teratomas showed varying degrees of resistance to the drug in vivo. Our findings suggest that the Chr1-eGSH is not suitable for therapeutic gene integration and highlight that topological analysis could facilitate exploration of human GSHs for regenerative medicine applications. Our data indicate that the HSV-TK/ganciclovir suicide gene approach alone may be not an adequate safeguard against the risk of teratoma, and suggest that the combination of several distinct approaches could reduce the risks associated with cell therapy. STEM CELLS TRANSLATIONAL MEDICINE 2019;8:627–638

SIGNIFICANCE STATEMENT

Tumorigenesis and the safety risks associated with genome editing are major concerns of human iPSC-based therapies. This report lists the features of human genome safe harbor candidates and demonstrates that topological and epigenetic analysis facilitates prediction of the influence of genome editing. This study also warns that the *HSV-TK* suicide gene system alone would not be an adequate safeguard. These data are helpful for developing a strategy to establish the safety of regenerative medicine in future. Thus, the work will contribute to solve the safety concerns for iPSC-based therapy.

INTRODUCTION

The development of human induced pluripotent stem cells (hiPSCs) has led to rapid advancements in the fields of disease modeling, gene therapy, drug discovery, and regenerative medicine [1, 2]. Recent advances in genome editing technologies, particularly the clustered regularly interspaced short palindromic repeats (CRISPR)/CRISPR-associated protein (Cas) system, have facilitated the targeted integration of functional DNA elements into the human genome,

thus, extending their research and therapeutic applications [3]. The future of hiPSC technology is quite promising, but there are some concerns that must be addressed prior to their broad clinical use.

A major concern related to hiPSC-based therapy is tumorigenicity [4]. Many approaches have been evaluated to address this issue [5]. One representative strategy is to equip cells with a suicide gene that can eliminate wayward tumor-initiating cells. This safeguard system has an advantage that a suicide gene can

be triggered even after cell transplantation or teratoma formation. This is of great value since mutations could occur in hiPSCs and their derivatives during culture [6] and differentiated cells could undergo malignant transformation. The most widely used gene is *herpes simplex virus thymidine kinase (HSV-TK)* that phosphorylates ganciclovir (GCV) and induces apoptosis by inhibiting DNA synthesis. It has a long history of use and its efficacy as a safeguard has been proven by previous studies [7–13]. However, a recent study documented the acquisition of GCV resistance by iPSCs expressing *HSV-TK* [14], although there were many differences in the experimental parameters. In previous studies, retroviral transduction was used to randomly insert suicide genes. Thus, the location where the transgenes were inserted and the number of inserted transgenes were not controlled, making it difficult to predict the behavior of transgenes and the risk of silencing upon hiPSC differentiation [15].

Another issue is the necessity to establish safe and robust ways to edit the human genome. The specificity of CRISPR-mediated genome editing techniques has improved [16–20]. However, we still do not know the location of true “genomic safe harbors (GSHs),” that is, the safest permissive loci to insert transgenes [21]. The *adeno-associated virus integration site 1 (AAVS1)* locus is most widely used as a GSH. However, recent studies have shown that this locus is not as safe and suitable as previously believed, since the transgene could disrupt the expression of *myosin binding subunit 85* [22] and could be silenced to variable degrees, due to epigenetic and other unknown mechanisms [23]. A detailed analysis of other candidate GSHs, such as the *chemokine (CC motif) receptor 5 (CCR5)*, *human ROSA26*, and some extragenic loci has not been fully performed. Therefore, the characterization of human GSH candidates is valuable as this knowledge will improve the safety of human cell engineering and cell-based therapies.

Recent advances in chromatin biology have permitted the elucidation of the three-dimensional genome architecture [24, 25]. One of the spectacular discoveries is that chromosomes are spatially partitioned into submegabase scale domains, often referred to as topologically associated domains (TADs) [26, 27]. Architectural proteins, such as the CCCTC-binding zinc finger protein (CTCF), associate with distant genomic regions and form loop structures. This structure brings genomic elements into close spatial proximity and facilitates interaction within an insulated domain [28]. Gene expression within a TAD is coordinated at the epigenetic level, indicating that TADs are essential functional units in the genome [29]. Thus, analysis of the TADs of GSH candidates will provide information to predict particularly prospective loci.

To address these two issues, we first analyzed the architecture of human GSH candidates. We then selected an extragenic GSH candidate on chromosome 1, knocked-in the *HSV-TK* gene using the CRISPR-Cas9 system, and investigated the behavior of transgenes and the feasibility of the HSV-TK/GCV system as a suitable safeguard against tumorigenicity for future hiPSC-based therapies.

MATERIALS AND METHODS

Animals

All animal care protocols and experiments were approved by the Laboratory Animal Research Department, Biomedical

Research Laboratory, Central Institute for Experimental Animals, Kawasaki, Japan.

Knockin Donor Vector Construction

The *HSV-TK* gene and P2A-Venus-polyA fragments was polymerase chain reaction (PCR) amplified from SFCMM-3 and pV-neoR vector [30]. These fragments, the human elongation factor-1 α (EF-1 α) promoter, IRES2 sequence, the puromycin resistant gene and homologous arms for knockin were inserted into the pBluescript II SK(+) plasmid using the ligation high (TOYOBO, Osaka, Japan) or in-Fusion HD cloning kit (Clontech, Mountain View, CA, USA). PCR primers are listed in Supporting Information Table S1.

CRISPR/Cas9 Nickase Plasmids

The bicistronic expression vector pX330-U6-Chimeric_BB-CBh-hSpCas9 (pX330, Addgene plasmid #42230) [31] was used to express Cas9 and a sgRNA. The Cas9-D10A nickase mutant vector (pX330-n) was created by site-directed mutagenesis of pX330 according to the protocol from Strategene. Targeting sequences of sgRNAs were designed using “Optimized CRISPR design” available at the Feng Zhang Laboratory website (<http://crispr.mit.edu/>). The sgRNA targeting sequences are listed in Supporting Information Table S2.

The Single Strand Annealing Assay

The genomic fragment containing the sgRNA targeting site was PCR amplified and inserted into pCAG-EGFP plasmids (addgene plasmid #50716) [32]. HEK293T cells were cultured in Dulbecco's modified Eagle's medium supplemented with 10% fetal bovine serum. 4×10^5 HEK293T cells were transfected with 1 μ g pCAG-EGFP plasmids and a pair of 0.75 μ g pX330-n plasmids using 15 μ g polyethylenimine. Enhanced green fluorescence protein (EGFP) fluorescence was assessed 48 hours after transfection. sgRNAs and PCR primers are listed in Supporting Information Tables S1 and S2.

Genome Editing of hiPSCs

Human iPSCs clone 409B2 were provided from the RIKEN cell bank (Tsukuba, Japan) [33]. hiPSCs were propagated by feeder-free system (mTeSR1 medium: STEMCELL Technologies, Vancouver, BC, Canada, and matrigel: Corning, Corning, NY, USA). Gene transfection was performed by 2 μ g of knockin donor plasmids, 1.5 μ g each of pX330-D10A Cas9 nickase plasmids and Amara Human Stem Cell Nucleofactor Kit using Amara nucleofactor (Lonza, Allendale, NJ) for 8×10^5 cells. For selection of stable lines, 0.5 μ g/ml puromycin was added to culture medium from 3 days after transduction. Puromycin resistant colonies were picked up after checked for venus expression by IX81 fluorescence microscopy (Olympus, Tokyo, Japan). Refer to Supporting Information for plasmid construction.

On-Target and Off-Target Analysis

Genomic DNAs were extracted using DNeasy Blood & Tissue Kit (Qiagen, Tokyo, Japan) according to manufacturer's instruction. Knockin and potential off-target sites were PCR amplified using primers listed in Supporting Information Table S1. Sequence of potential off-target sites were checked by direct sequencing or pGEM-T easy vector systems (Promega, Madison, WI).

In Vitro Differentiation (Embryoid Body Formation)

hiPSCs were seeded into an ultra-low attachment 96-well plate (Sumitomo Bakelite Co., Ltd., Tokyo, Japan) at a density of 1×10^4 cells per well and cultured in bFGF-free knockout serum replacement based hES medium for differentiation into embryoid bodies (EBs).

Transcript Analyses

Total RNAs of cultured cells and teratoma tissues were isolated using QIAzol (Qiagen, Tokyo, Japan). cDNAs were synthesized using PrimeScript RT reagent Kit (Takara Bio Inc., Shiga, Japan). The expression of *HSV-TK* gene was confirmed by quantitative PCR (qPCR) with AmpliTaq Gold 360 Master Mix (Thermo Fisher Scientific, Waltham, MA, USA) using GeneAmp PCR System 9700 (Thermo Fisher Scientific). Analysis of reverse transcription qPCR (RT-qPCR) was performed using TaqMan Array Human Stem Cell Pluripotency Panel or gene specific primers (Supporting Information Table S3) and Power SYBR Green PCR Master Mix using QuantStudio 12K Flex real-time PCR system (Thermo Fisher Scientific). Statistical significance of *HSV-TK* expression in teratomas was determined using Kruskal–Wallis analysis of variance (ANOVA).

In Vitro Cytotoxicity Assay

Cytotoxic activity on knockin hiPSCs was determined as the following. *HSV-TK* knockin cells and their parent hiPSCs were seeded into a Matrigel coated 96-well plate at a density of 5×10^3 cells per well. On day 2, GCV was applied at 0, 10^{-4} , 10^{-3} , 10^{-2} , 0.1, 1.0, 10, and 100 μM . After 48 hours, ATP content was determined using the Celltiter-Glo reagent (Promega, Madison, WI, USA) according to the manufacturer's instructions. Luminescence was determined on a 2030 ARVO X5 (PerkinElmer, Norwalk, CT). Cytotoxic activity on embryoid bodies (EBs) was determined as the following. GCV was administered at 0, 10^{-3} , 10^{-2} , 0.1, 1.0, and 10 μM from day 1 at every other day. Images of EBs at day 7 were analyzed by ImageJ software to measure Feret diameter for an estimate of EB volume. Fifty percentage lethal concentration (LC_{50}) values of in vitro cytotoxicity assay were obtained using analysis of dose–response curves (drc) package in R (<https://www.R-project.org/>) by fitting two-parameter log-logistic curves to each combination of GCV concentration and cell viability [34].

In Vivo Teratoma Assay

NOG (NOD/Shi-scid IL2Rgnull) mice, aged 6–8 weeks, were maintained under specific-pathogen-free conditions in the Animal Center of the Central Institute for Experimental Animals in accordance with the guidelines of the facility. The recipient mice were anesthetized by inhalation of isoflurane (Dainippon Pharmaceutical Co., Ltd., Japan, Osaka). For subcutaneous transplantation, *HSV-TK* knockin hiPSCs (TK#1–3, $3\text{--}5 \times 10^5$ cells) suspended in 0.1 ml of a 1:1 mixture of growth factor reduced Matrigel (BD Bioscience, San Jose, CA, USA) and Williams' Medium E (Thermo Fisher Scientific), were subcutaneously inoculated into mice. The mice were monitored daily and the teratomas were measured using calipers. Teratoma volume (TV) was calculated using the formula $\text{TV} = \frac{1}{2} \times A \times B^2$ (A : length [mm]; B : width [mm]). The criteria for successive engraftment were as follows: progressive nodule growth at the site of injection and TV values exceeding 10 mm^3 . After 5 weeks,

0.2 mg/ml of valganciclovir (Sigma–Aldrich, St. Louis, MO, USA) or saline (Otsuka Pharmaceutical, Tokyo, Japan) was added to the drinking water. At 21–25 days after GCV or vehicle administration, teratomas were recovered from the sacrificed mice.

Statistical Analyses of the In Vivo Teratoma Assay

The sequential results of TV were statistically analyzed using two-way ANOVA after the GCV group was divided into two groups by teratoma growth rate. One week before the endpoint, individuals with a rate of volume increase within 300% of the start point were designated the effective group, whereas individuals with a higher growth rate were designated the non-effective group.

Immunohistochemistry

Teratomas were fixed with Mildform 10NM formaldehyde solution (FUJIFILM Wako Pure Chemical Corporation, Osaka, Japan). Formalin-fixed tissues were embedded in paraffin and then sliced and analyzed by either hematoxylin–eosin (H&E) staining or immunohistochemistry. The following antibodies were used for immunohistochemistry: mouse anti-human leukocyte antigen (clone: EMR8-5, Hokudo, Sapporo, Japan) and mouse anti-Ki67 (clone: MIB-1, Dako, Glostrup, Denmark). Immunostaining was performed with Leica Bond-Max automatic immunostainer (Leica Biosystems, Mount Waverley, VIC, Australia). Paraffin sections were dewaxed in a Bond Dewax solution and rehydrated in alcohol and Bond Wash solution (Leica Biosystems). Antigen retrieval was performed using a 10 mM citrate buffer, pH 6 (ER1) retrieval solution, followed by endogenous peroxidase blocking on the machine. Detection was performed using the Bond Polymer Refine Detection system. Sections were then counterstained with hematoxylin on the machine.

DNA Methylation Analyses

CpG islands, regions with a high frequency of 5'-C-phosphate-G-3' (CpG) sequences of nucleotides, in the EF-1 α promoter were identified using EMBOSS Cpgplot (https://www.ebi.ac.uk/Tools/seqstats/emboss_cpplot/) with the following criteria; observed to expected ratio of C + G to CpG > 0.60, percentage of G + C > 50, and length > 200 nt. DNA methylation of the CpG island of the EF-1 α promoter was analyzed by pyrosequencing using the PyroMark Q24 advanced system (Qiagen) after the bisulfite-conversion of genomic DNA using the EZ DNA Methylation-Gold Kit (Zymo Research, Irvine, CA). Primers were designed using PyroMark Assay Design (Qiagen) and are listed in Supporting Information Table S4. The DNA methylation status of the 10 CpG sequences in the EF-1 α promoter region was described as a percentage (%).

Epigenetic Analysis

The topological architecture and an automated computational system for learning chromatin states, ChromHMM, were analyzed using the WashU epigenome browser (ref seq, hg19) [35, 36]. The CTCF chromatin interaction analysis dataset by paired-end tag sequencing (ChIA-PET) data for GM12784 was obtained from a previous study [28]. CTCF motif orientation was obtained from GSE63525 and was added to the track [37]. The ChIA-PET data for K562 and MCF-7 was obtained from the ENCODE data repository [38]. ChromHMM information was generated using the ENCODE project dataset [38, 39].

RESULTS

Topological Architecture of Human GSH Candidates

To determine the feasible loci for transgene introduction, we analyzed the CTCF ChIA-PET and depicted the topological architecture of human GSH candidates [36, 38]. We also analyzed the CTCF motif sites and orientation because the two boundaries of many TADs contain multiple binding sites for CTCF with convergent orientation where CTCF also contributes to connect distant genomic areas within TADs [37]. An extragenic GSH candidate on chromosome 1 (Chr1-eGSH) is one of the GSH candidates located far from any gene, microRNA loci, and ultra-conserved regions. Importantly, this locus permitted the expression of a lentivirus encoded β -globin transgene in hiPSCs and their erythroid progeny [40]. CTCF ChIA-PET showed that the Chr1-eGSH might be within a broad TAD (Fig. 1A, Supporting Information Fig. S1). There was no annotated gene within the closest CTCF-loop domain. However, an integrated transgene could possibly interact with *BMP/Retinoic Acid Inducible Neural-Specific Protein 3 (BRINP3)* located at a distance of 2 Mb. *Phospholipase A2 group IVA (PLA2G4A)* located at the 5' side is topologically separated from the Chr1-eGSH TAD. The innermost CTCF-loop of the *AAVS1* locus contained only *Protein phosphatase 1 regulatory subunit 12C (PPP1R12C)*, but transgenes could interact with neighboring genes including cancer-related genes such as *Receptor-type tyrosine-protein phosphatase H (PTPRH)* and *NACHT, LRR, and PYD domains-containing protein 2 (NLRP2)*; Supporting Information Fig. S1). The *CCR5* locus showed strong CTCF interactions and inserted transgenes could affect *CCR1*, *CCR2*, and *CCR3*. This is consistent with the results of a previous study that showed that a transgene in the *CCR5* locus upregulated *CCR1* expression [41]. Likewise, manipulation of the *human ROSA26* locus may influence the expression of nearby genes, especially *THUMP domain-containing protein 3 (THUMPD3)* and *SET domain containing 5 (SETD5)*. An automated computational system for learning chromatin states, ChromHMM [39], suggested that the Chr1-eGSH locus was relatively quiescent compared with other GSH candidates and was not in a repressive state (Supporting Information Fig. S2). Therefore, the Chr1-eGSH locus was considered a safe and permissive locus, and we used this locus for the insertion of *HSV-TK*.

The Extragenic Safe Harbor Permitted *HSV-TK* Expression in Knockin hiPSCs

To examine how a newly integrated promoter/transgene behaves in the Chr1-eGSH locus and whether the *HSV-TK/GCV* suicide system works as a safeguard against tumorigenesis, we generated knockin hiPSCs harboring *HSV-TK* using the CRISPR/Cas9 method (Fig. 1B, 1C). Homologous arms for the knockin were designed in the Chr1-eGSH topologically insulated domain at a distance of 50 kb from the original integration site [40] since the original position was near the CTCF anchor site, where it could possibly be influenced by interactions with other CTCF anchoring zones [24].

To edit the human genome using the CRISPR/Cas9 technique, we combined the double nicking strategy and truncated single guide RNAs (sgRNAs) to reduce the risk of off-target mutagenesis [30]. On-target cleavage activity of full-length and truncated sgRNAs was assessed by the single strand annealing

assay, and 20–17 nt and 19–17 nt sgRNA pairs were identified for use in the induction of double nicks on the Chr1-eGSH locus (Supporting Information Fig. S3). The hiPSCs were then electroporated with donor vectors and Cas9 nickase/sgRNA expressing vectors. A pair of Cas9 nickases created a double strand break in the target genome site, followed by knockin of the EF-1 α -*HSV-TK*-IRES-puromycin resistant gene-P2A-Venus cassette by homology-directed repair. After electroporation, cells were cultured under puromycin selection. Individual puromycin resistant hiPSC clones were recovered. Six out of 16 lines possessed the knockin allele (Fig. 1D, Supporting Information Fig. S3). From these, we used three knockin clones, TK#1–3, for further experiments (Fig. 1E). Next, we investigated whether off-target mutations accompanied genome editing. There were no potential off-target double nicking pairs. Since nick-mediated double strand breaks could occur and lead to off-target indel mutations, we checked the top five off-target candidates of each sgRNA and confirmed that no obvious mutations were observed in the three knockin hiPSC lines (Supporting Information Fig. S3). Three independent knockin hiPSC clones showed uniform, high-level *HSV-TK* expression driven by the human EF-1 α promoter, a constitutive promoter of human origin (Fig. 1F). Since CTCF ChIA-PET analysis suggested that *BRINP3* is possibly located within the Chr1-eGSH TAD (Fig. 1A, Supporting Information Fig. S1), we also investigated *BRINP3* expression. *BRINP3* expression slightly increased in the three knockin iPSCs, whereas there were no obvious alterations in the expression of *PLA2G4A* which is located outside the Chr1-eGSH TAD (Fig. 1G).

Therefore, we established *HSV-TK* knockin hiPSCs with a reduced risk of off-target mutations. The Chr1-eGSH locus was permissive for transgene expression, although a gene located at a distance of 2 Mb in the same TAD might be affected.

***HSV-TK/GCV* Eliminated the Knockin Cells In Vitro**

We next investigated the cytotoxic effect of GCV on *HSV-TK* knockin cells. Knockin hiPSCs were highly sensitive to GCV exposure in vitro (Fig. 2A). The in vitro LC₅₀ of wild type (WT) and TK#1–3 was 203 μ M, 0.043 μ M, 0.048 μ M, and 0.074 μ M, respectively. Almost all knockin cells died by 48 hours after 10 μ M GCV treatment. Since *HSV-TK/GCV* exerts a cytotoxic effect by disturbing DNA synthesis, actively proliferating cells may be more sensitive to this suicide system. To test this notion, we differentiated hiPSCs through EB formation for 7 days and treated the EBs with GCV for another 3 days (Fig. 2B). GCV exposure reduced the relative *OCT3/4* expression in EBs formed by *HSV-TK* knockin cells, suggesting that GCV preferentially killed the remaining *OCT3/4*-positive cells or enhanced their differentiation. Next, we formed EBs under various GCV concentration. Under these conditions, the size of EBs was significantly reduced as expected (Fig. 2C, 2D). LC₅₀ of EBs from TK#1, TK#2, and TK#3 was 0.018 μ M, 0.005 μ M, and 0.01 μ M, respectively. The marker gene expression of all three embryonic-germ layers was increased in GCV-treated EBs compared with that in untreated EBs (Fig. 2E). This result indicated that knockin hiPSCs were capable of differentiating into the three embryonic-germ lineages and that the remaining stem cells were preferentially ablated or differentiated by *HSV-TK/GCV* treatment. Notably, *HSV-TK* expression was not altered even though the cell population of EBs was changed, suggesting that the Chr1-eGSH locus permitted stable *HSV-TK* expression at least during early

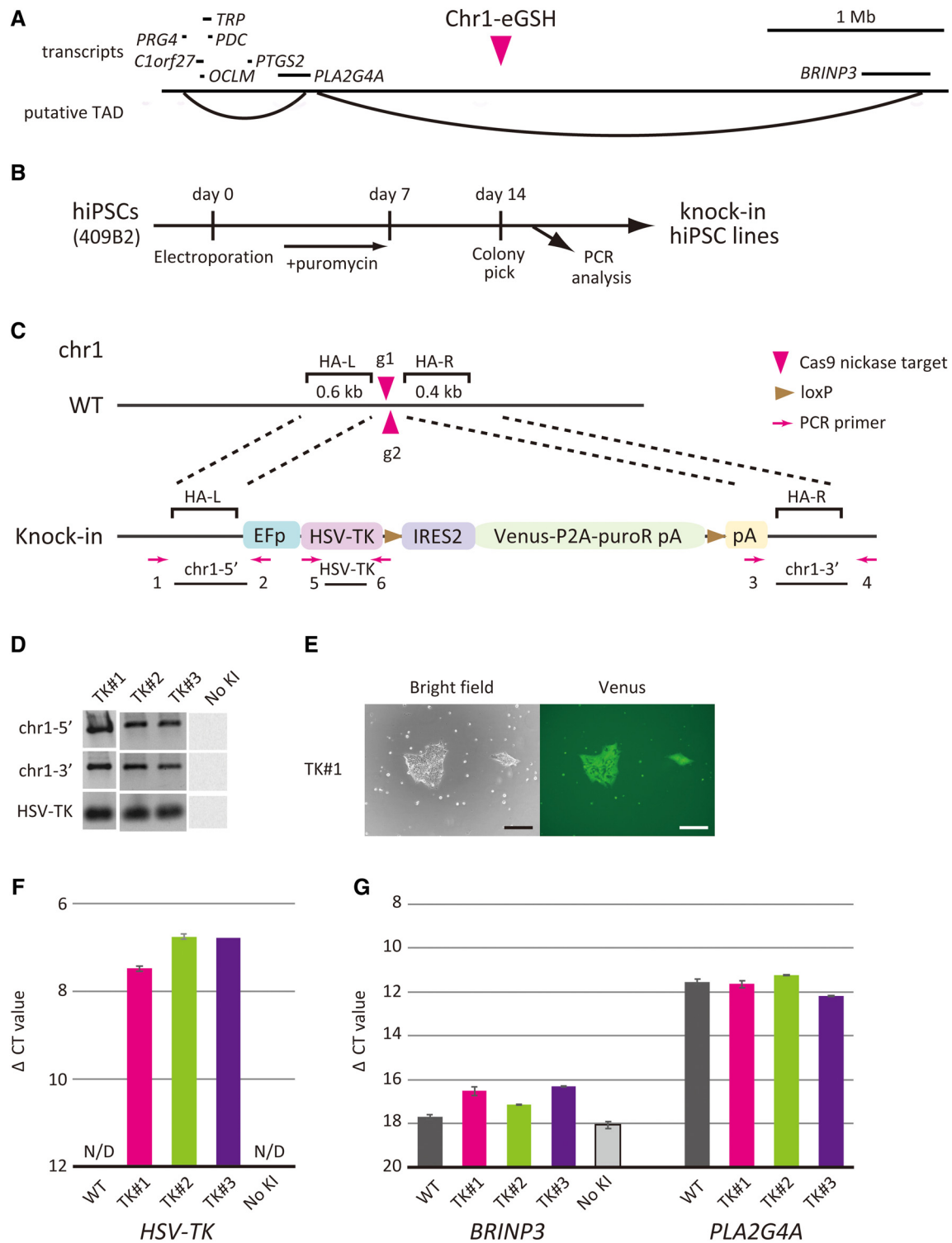


Figure 1. Generation of knockin hiPSCs carrying the *HSV-TK* transgene at the Chr1-eGSH locus. **(A):** Topological architecture of an extragenomic genomic safe harbor on chromosome 1 (Chr-eGSH). Transcripts and putative topologically associated domains are shown. **(B):** Experimental flow to create knockin human induced pluripotent stem cells (hiPSCs). **(C):** Schematic illustration of the WT and knockin alleles. The left and right homologous arms are indicated as HA-L and HA-R, respectively. The PCR primers used are shown as magenta arrows. **(D):** Targeted knockin of the *HSV-TK* cassette detected by genomic PCR. No KI is an iPSC clone electroporated with vectors but without *HSV-TK*. The results for all isolated clones are shown in Supporting Information Figure S3. **(E):** Bright field and fluorescence images of the representative knockin iPSC line (TK#1). Scale bar: 100 μ m. **(F):** *HSV-TK* expression levels in WT and knockin iPSCs. Relative expression to *GAPDH* (delta CT value) is shown. Data are represented as mean \pm SD ($n = 3$ for each line). **(G):** Relative expression levels of 5' and 3' proximate genes in WT and knockin iPSCs. Relative expression to *GAPDH* (delta CT value) is shown. Data are represented as the mean \pm SD ($n = 3$ for each line). Abbreviations: EFp, human elongation factor-1 α promoter; HSV-TK, herpes simplex virus thymidine kinase; IRES2, internal ribosomal entry site 2; N/D, not detected; pA, poly A; puroR, puromycin resistant gene.

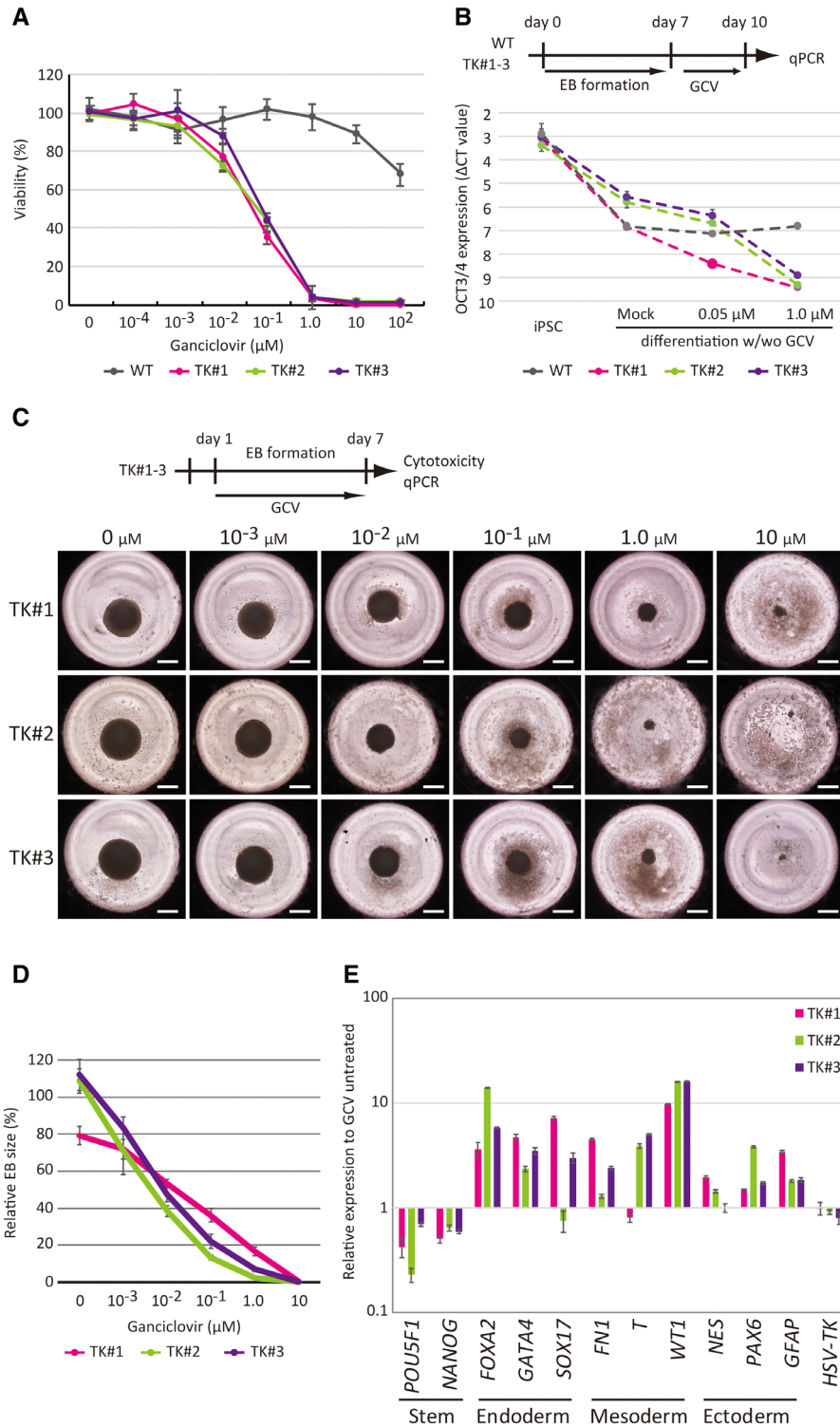


Figure 2. Herpes simplex virus thymidine kinase (HSV-TK)/ganciclovir eliminates knockin human induced pluripotent stem cells (hiPSCs). **(A):** in vitro cytotoxicity assay of WT and knockin hiPSCs. Cell viability was evaluated 48 hours after ganciclovir treatment at the indicated concentration. LC₅₀ of 409B2, TK#1, TK#2, and TK#3 was 203 μM , 0.043 μM , 0.048 μM , and 0.074 μM , respectively. Data are represented as mean \pm SD ($n = 6$ for each line). **(B):** Cytotoxic effect of ganciclovir on *OCT3/4* positive cells upon in vitro differentiation. The upper scheme shows the experimental flow. *OCT3/4* expression was analyzed by qPCR at day 9 and was normalized to *GAPDH* expression. Data are represented as the mean \pm SD ($n = 3$ for each line). **(C):** Effect of ganciclovir on embryoid body (EB) formation. Images at day 7 are shown. Scale bar: 250 μm . **(D):** Cytotoxic effect of ganciclovir on EBs. The volume of EBs at day 7 was analyzed. Data are represented as the mean \pm SD ($n = 8$ for each line). LC₅₀ of TK#1, TK#2, and TK#3 was 0.018 μM , 0.005 μM , and 0.01 μM , respectively. **(E):** Relative expression levels of lineage marker genes and *HSV-TK* in EBs formed in the presence and absence of ganciclovir treatment. Marker gene expression of 0.1 μM GCV-treated EBs was compared with that of untreated EBs. Relative expression levels were normalized to *GAPDH* expression levels. Data are represented as mean \pm SD ($n = 3$ for each line).

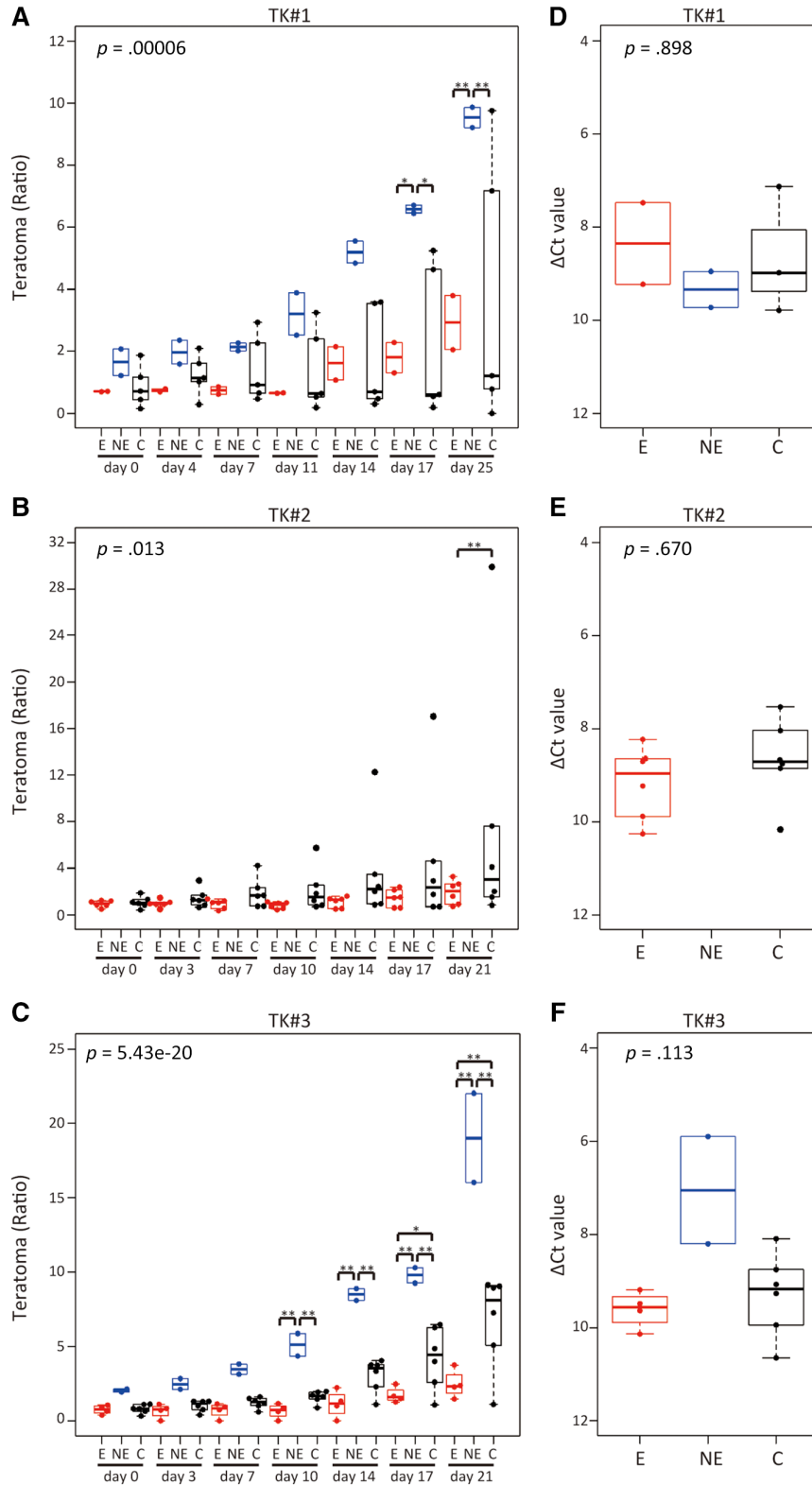


Figure 3. In vivo teratoma assay. (A–C): Tumoricidal effects of herpes simplex virus thymidine kinase (HSV-TK)/ganciclovir (GCV) on established teratomas formed by TK#1 (A), TK#2 (B), or TK#3 (C) knockin human induced pluripotent stem cells (hiPSCs). The size (relative area) of each tumor was compared with that before GCV or vehicle injection. Size relative to the average start volume is shown. GCV treated teratomas were divided into an effective group and a non-effective group. Statistical significance was determined using two-way analysis of variance (ANOVA). *, $p < .05$; **, $p < .01$. (D–F): Relative expression levels of *HSV-TK* in TK#1 (D), TK#2 (E), or TK#3 (F) teratomas. Relative expression levels were normalized to *GAPDH* expression levels. Statistical significance was determined using Kruskal–Wallis ANOVA. Abbreviations: E, effective; NE, non-effective; C, control.

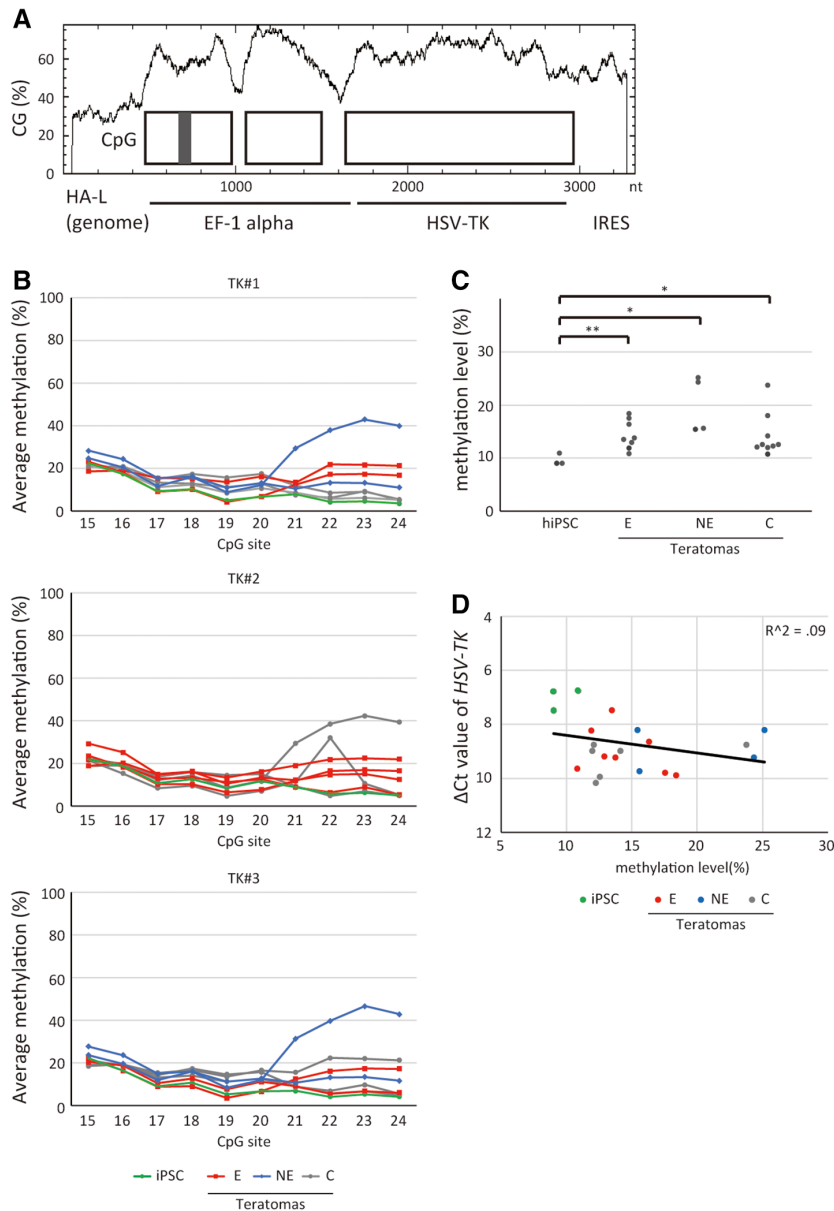


Figure 4. DNA methylation analyses of the promoter. **(A):** CpG islands of the EF-1 α promoter and *HSV-TK* transgene. CpG islands are indicated by boxes, with a gray box indicating the CpGs analyzed. **(B):** The average DNA methylation level of each CpG site. **(C):** Mean DNA methylation levels of the analyzed CpGs of human induced pluripotent stem cells and teratomas. Statistical significance was determined using the Student's *t* test. *, $p < .05$; **, $p < .01$. **(D):** Correlation between the DNA methylation of the EF-1 α promoter and *HSV-TK* expression. Relative expression levels of *HSV-TK* were normalized to *GAPDH* expression levels. The Pearson's correlation coefficient is shown. Abbreviations: C, control teratomas; E, effective teratomas; HA-L, left homologous arm for knockin; NE, noneffective teratomas.

differentiation (Fig. 2E). Therefore, these results indicated that the Chr-eGSH locus may permit stable *HSV-TK* expression and that GCV eliminated the knockin cells in vitro.

Tumoricidal Effect of HSV-TK/GCV Was Insufficient as a Safeguard Against Established Teratomas

We next tested whether *HSV-TK* inserted in the Chr1-eGSH locus abolished tumor cells in vivo. Suicide gene approaches have the advantage of being able to exert a cytotoxic effect after cell transplantation. In clinical settings, it is conceivable

that GCV is administered when a tumor is detected by follow-up imaging tests after transplantation. Therefore, we investigated the tumoricidal effect of *HSV-TK*/GCV on preformed teratomas. We subcutaneously injected the *HSV-TK* knockin hiPSCs into NOG mice. Five weeks later, teratomas became palpable. Thereafter, valganciclovir or saline was administered in the drinking water, and tumor size was monitored (Fig. 3A, 3C, Supporting Information Fig. S4, Supporting Information Table S5). All teratomas formed by TK#2 were sensitive to GCV treatment, although the size of teratomas slowly increased

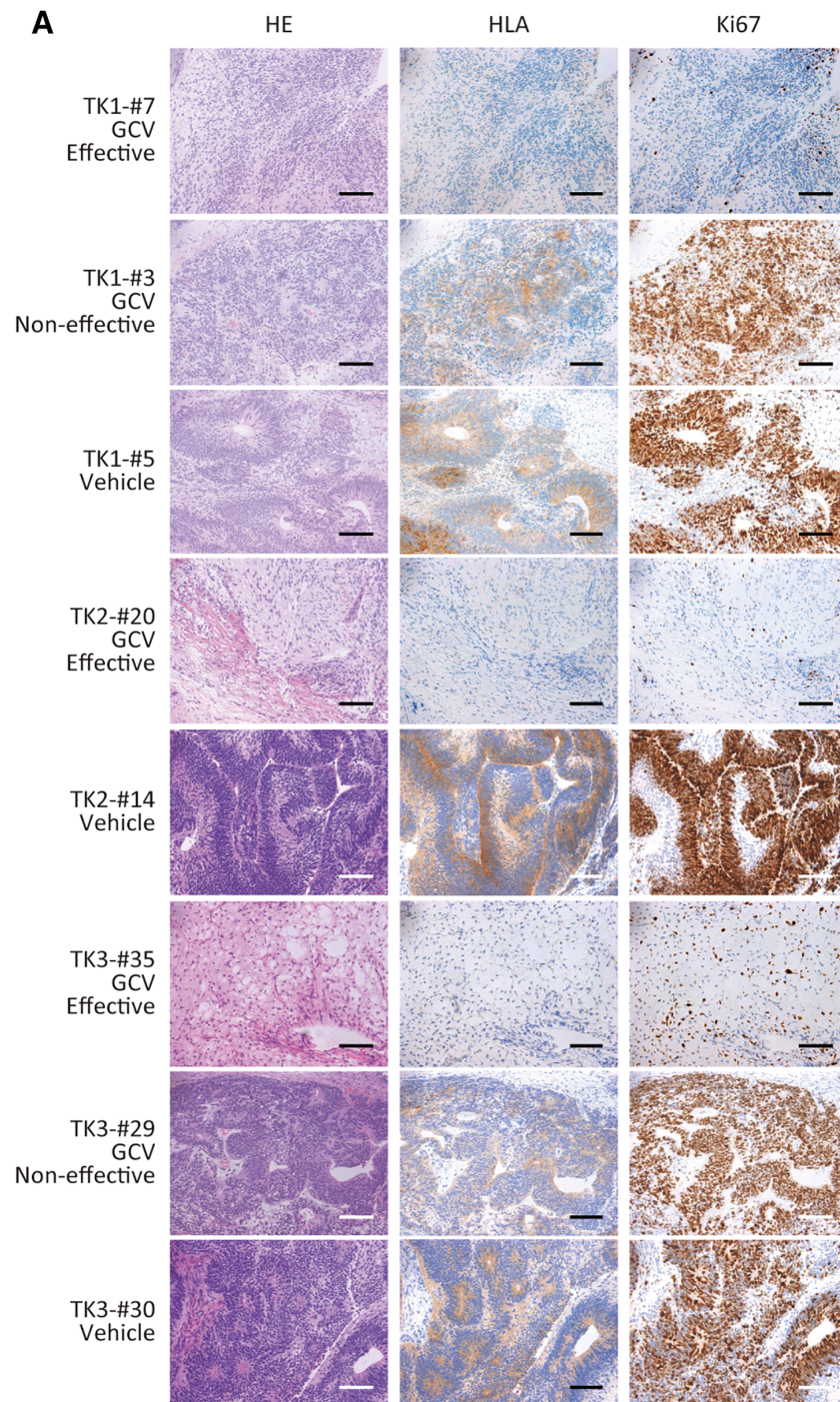


Figure 5. Histological analysis of teratomas. Histological analysis of the injection sites in ganciclovir or vehicle treated teratomas. Representative images are shown. Scale bar: 100 μ m.

during the observation period (Fig. 3B, Supporting Information Fig. S4). Notably, teratomas derived from TK#1 and TK#3 were classified into both the GCV effective group and the GCV non-effective group even though they had the same genetic background (Fig. 3A, 3C). The size of the GCV effective teratomas slowly increased as for TK#2 teratomas (Supporting Information Fig. S4). We noted a variety of teratoma sizes in the vehicle-treated group, indicating the heterogeneity of teratomas derived from the same hiPSC clone.

To investigate whether the silencing or gene disruption of *HSV-TK* caused GCV resistance, we first measured the *HSV-TK* expression of teratoma cells using qPCR. There was no significant difference between the *HSV-TK* expression of the GCV effective, GCV noneffective, and control groups (Fig. 3D, 3E). Rather, the *HSV-TK* expression of the GCV noneffective teratomas formed by TK#3 tended to be higher than that of the GCV effective teratomas. Next, we analyzed the DNA methylation of the CpG island of the EF-1 α promoter by pyrosequencing

(Fig. 4A), as silencing of a transgene is accompanied by DNA methylation of its promoter [42]. The DNA methylation levels of the promoter were low in knockin hiPSCs and teratomas (Fig. 4B). No significant difference was observed between the GCV effective, GCV noneffective, and control teratomas, although teratomas showed higher DNA methylation levels than their parent knockin hiPSCs (Fig. 4C). There was no correlation between DNA methylation and *HSV-TK* expression under these low DNA methylation levels (Fig. 4D). These data suggested that *HSV-TK* silencing may not be the main cause of random GCV effect.

Finally, we analyzed the injection sites in GCV- or vehicle-treated teratomas. Few HLA-positive or Ki-67 positive cells were found at the injection sites in GCV sensitive cases (Fig. 5). In contrast, we found an increased number of HLA- and Ki-67 positive, that is, proliferating human cells at the injection sites in GCV resistant cases. These GCV resistant teratomas were histologically comparable to those in the vehicle-treated mice. Although tumoricidal effects were observed, these data indicated that the insertion of *HSV-TK* into the Chr1-eGSH locus was not sufficient to eliminate established solid teratomas in vivo.

DISCUSSION

Here, we analyzed the topological feature of representative human GSH candidates and evaluated one of the extragenic GSH candidates by *HSV-TK* insertion. The *HSV-TK* transgene was highly expressed in the Chr1-eGSH locus, but possibly affected the expression level of *BRINP3*, which is located at a distance of 2 Mb within the same TAD (Fig. 1A, 1G). The insertion of the promoter/transgene cassette into the same TAD, or *HSV-TK* expression itself, might affect *BRINP3* expression. However, the expression level of *BRINP3* was low in iPSCs, therefore, we cannot exclude the possibility that this result was an artifact. Nevertheless, the Chr1-eGSH locus may not be a suitable locus for therapeutic gene integration, as *BRINP3* could be associated with pituitary gonadotropinomas [43] and inflammation [44]. Notably, CTCF ChIA-PET analysis predicted this distant interaction, which has not been previously reported [40]. Although we used a public ChIA-PET dataset which was not generated from hiPSCs, our results suggested that bioinformatics approaches could be powerful tools for exploring the ideal human GSH and predicting the effect of genome editing.

We also assessed the effect of the HSV-TK/GCV safeguard system against preformed teratomas since malignant transformation of administered cells could occur after transplantation. The suicide gene system tested here would be not feasible for critical tissue transplantation or cell transplantation into critical organs, since removal of transplanted cells would be disastrous for patients. In addition, the destruction of wayward transplanted cells could damage neighboring normal cells in the recipient due to the bystander effect of the HSV-TK/GCV system. However, when the transplanted tissues are not critical or can be supported until retreatment, a suicide gene driven by a constitutive promoter will be applicable as a safeguard. Examples may include cell transplantation into non-critical organs, pancreatic islet transplantation for severe diabetes mellitus [45], mini liver transplantation for liver failure

or inherited liver enzyme deficiency [46] and bioartificial kidneys for patients receiving dialysis [47]. Unlike the purge of undifferentiated cells before transplantation [48, 49], the suicide gene approach can be activated after transplantation and has the potential to kill metastases in case of malignant transformation. Thus, the evaluation and development of a feasible suicide gene system will be important for future regenerative medicine.

The in vivo tumoricidal effects of HSV-TK/GCV varied and were not adequate in our study, although the insertion of EF-1 α -*HSV-TK* in the Chr1-eGSH locus efficiently eliminated knockin hiPSCs in vitro (Figs. 3, 5, Supporting Information Fig. S4). Previous studies have demonstrated that the HSV-TK/GCV suicide system ablated teratomas in an efficient and specific manner [7–13]; however, one recent study reported GCV resistance partially due to escape mutations in *HSV-TK* [14]. The experimental parameters differed between these studies, including the iPSC or embryonic stem cell (ESC) lines, cell preparation, promoter, gene integration method, *HSV-TK* variant, onset and duration of GCV treatment after cell transplantation, GCV dose, route of GCV administration, and observation period. This diversity could explain the different outcomes. Ours was the only study to use the knockin method to insert *HSV-TK* into the host genome. This method can control the integration site and reduces the risk of epigenetic silencing by proviral sequences [42]; however, only one or two cassettes can be inserted into the genome. In contrast, viral transfection can result in multiple *HSV-TK* copies when cells are transduced at a high multiplicity of infection, and clones strongly expressing *HSV-TK* are selected. Thus, the *HSV-TK* expression level in our study could be lower than in previous studies, and may be one reason why we failed to eliminate teratomas in vivo.

Another potential cause of GCV resistance is the epigenetic silencing of the EF promoter or *HSV-TK*. This may be not the main cause in our study since the DNA methylation level in teratomas was low, and GCV noneffective teratomas showed equal or higher *HSV-TK* expression than GCV effective teratomas (Figs. 3D–3F, 4). However, there is a possibility that teratoma formation reduced *HSV-TK* expression and led to the discrepancy between in vitro and in vivo tumoricidal effects (Fig. 4D). As our hiPSCs may only carry one *HSV-TK* gene, the transgene may have been more vulnerable to such situations here than in previous studies in which cells may have multiple transgenes at multiple loci.

The variability between hiPSC lines could also affect the results, as each study used different iPSC or ESC lines. Considering the differences in their genetic and epigenetic backgrounds, cell line choice may affect the sensitivity to GCV treatment. The knockin hiPSCs we used were sensitive to GCV before injection, whereas teratomas showed various responses to GCV even though they had the same genetic and epigenetic background when injected (Fig. 3). This suggests that GCV resistance may not be solely attributed to the cell line we used, and we propose that host factors such as the vascularization and/or cell contents of teratomas also influenced in vivo GCV susceptibility. These factors are difficult to control and should be taken into consideration when using suicide gene approaches against tumorigenesis in future regenerative medicine.

Another suicide gene system, such as iCaspase-9/AP20187, could be more promising as a safeguard for tumorigenesis

after transplantation [49, 50]. However, this system may not be available in hematopoietic stem cell engraftment as non-specific toxicity of AP20187 on hiPSCs and CD34⁺ cells have been reported [49]. Considering that escape mutations could take place and that the tumoricidal effect of the suicide gene approaches could not reach 100%, combination of suicide gene systems with selection methods before transplantation including cell sorting [51] and small molecules to purge undifferentiated iPSCs [48, 49] may reduce the risks of tumor formation associated with cell therapy.

CONCLUSION

We list the topological features of the human genome safe harbor candidates and demonstrate that bioinformatics analysis facilitates prediction of the influence of genome editing. *HSV-TK* inserted in the Chr1-eGSH locus was not sufficient to eliminate established teratomas in vivo. The in vitro GCV sensitivity did not predict the in vivo response of teratomas to GCV treatment. The tumoricidal effects of GCV varied among teratomas, suggesting that other unknown variables influenced the outcome. Therefore, careful evaluation will be required before applying the HSV-TK/GCV safeguard approach to regenerative medicine.

ACKNOWLEDGMENTS

This work is supported by JSPS KAKENHI Grant Number JP16K19511 for Y. Kimura, and JP15K15534 for Y. Kanemura, and the Research Center Network for Realization of Regenerative Medicine from Japan Agency for Medical Research and Development, AMED for Y. Kanemura. We thank Editage (www.editage.jp) for English language editing.

REFERENCES

- 1 Takahashi K, Tanabe K, Ohnuki M et al. Induction of pluripotent stem cells from adult human fibroblasts by defined factors. *Cell* 2007;131:861–872.
- 2 Shi Y, Inoue H, Wu JC et al. Induced pluripotent stem cell technology: A decade of progress. *Nat Rev Drug Discov* 2017;16:115–130.
- 3 Komor AC, Badran AH, Liu DR. CRISPR-based technologies for the manipulation of eukaryotic genomes. *Cell* 2017;168:20–36.
- 4 Lee AS, Tang C, Rao MS et al. Tumorigenicity as a clinical hurdle for pluripotent stem cell therapies. *Nat Med* 2013;19:998–1004.
- 5 Jeong HC, Cho SJ, Lee MO et al. Technical approaches to induce selective cell death of pluripotent stem cells. *Cell Mol Life Sci* 2017;74:2601–2611.
- 6 Klawitter S, Fuchs NV, Upton KR et al. Reprogramming triggers endogenous L1 and Alu retrotransposition in human induced pluripotent stem cells. *Nat Commun* 2016;7:10286.
- 7 Schuldiner M, Itskovitz-Eldor J, Benvenisty N. Selective ablation of human embryonic stem cells expressing a “suicide” gene. *STEM CELLS* 2003;21:257–265.
- 8 Jung J, Hackett NR, Pergolizzi RG et al. Ablation of tumor-derived stem cells transplanted to the central nervous system by genetic modification of embryonic stem

cells with a suicide gene. *Hum Gene Ther* 2007;18:1182–1192.

9 Cheng F, Ke Q, Chen F et al. Protecting against wayward human induced pluripotent stem cells with a suicide gene. *Biomaterials* 2012;33:3195–3204.

10 Rong Z, Fu X, Wang M et al. A scalable approach to prevent teratoma formation of human embryonic stem cells. *J Biol Chem* 2012;287:32338–32345.

11 Chen F, Cai B, Gao Y et al. Suicide gene-mediated ablation of tumor-initiating mouse pluripotent stem cells. *Biomaterials* 2013;34:1701–1711.

12 Tieng V, Cherpin O, Gutzwiller E et al. Elimination of proliferating cells from CNS grafts using a Ki67 promoter-driven thymidine kinase. *Mol Ther Methods Clin Dev* 2016;6:16069.

13 Sulkowski M, Konieczny P, Chlebanowska P et al. Introduction of exogenous HSV-TK suicide gene increases safety of keratinocyte-derived induced pluripotent stem cells by providing genetic “Emergency Exit” Switch. *Int J Mol Sci* 2018;19:197.

14 Kotini AG, de Stanchina E, Themeli M et al. Escape mutations, ganciclovir resistance, and teratoma formation in human iPSCs expressing an HSVtk suicide gene. *Mol Ther Nucleic Acids* 2016;5:e284.

15 Fontes A, Lakshminpathy U. Advances in genetic modification of pluripotent stem cells. *Biotechnol Adv* 2013;31:994–1001.

AUTHOR CONTRIBUTIONS

Y. Kimura: conception and design, financial support, collection, analysis and interpretation of data, manuscript writing, final approval of manuscript; T.S., Y.H., D.K., A.Y., A.K.: collection, analysis and interpretation of data, final approval of manuscript; I.N., M. Oda: data analysis and interpretation, final approval of manuscript; M.N.: conception and design, final approval of manuscript; M. Onodera: data interpretation, final approval of manuscript; H.S., Y. Kanemura: financial support, collection, analysis and interpretation of data, final approval of manuscript; T.N.: financial support, data interpretation, final approval of manuscript; H.M.: conception and design, analysis and interpretation of data, final approval of manuscript.

DISCLOSURE OF POTENTIAL CONFLICTS OF INTEREST

H.M. declared research funding by the Brain Mapping by Integrated Neurotechnologies for Disease Studies (Brain/MINDS) from Japan Agency for Medical Research and development, AMED; Grant-in-Aid for Scientific Research on Innovative Areas (Brain Protein Aging and Dementia Control; 17H05700) from MEXT” and AMED under Grant Number 17km0405206h0002. The other authors indicated no potential conflicts of interest.

DATA AVAILABILITY STATEMENT

The data that support the findings of this study are available from the corresponding author upon request.

16 Ran FA, Hsu PD, Lin CY et al. Double nicking by RNA-guided CRISPR Cas9 for enhanced genome editing specificity. *Cell* 2013;154:1380–1389.

17 Fu YF, Sander JD, Reyon D et al. Improving CRISPR-Cas nuclease specificity using truncated guide RNAs. *Nat Biotechnol* 2014;32:279–284.

18 Shen B, Zhang W, Zhang J et al. Efficient genome modification by CRISPR-Cas9 nickase with minimal off-target effects. *Nat Methods* 2014;11:399–402.

19 Kleinstiver BP, Pattanayak V, Prew MS et al. High-fidelity CRISPR-Cas9 nucleases with no detectable genome-wide off-target effects. *Nature* 2016;529:490–495.

20 Fellmann C, Gowen BG, Lin PC et al. Cornerstones of CRISPR-Cas in drug discovery and therapy. *Nat Rev Drug Discov* 2017;16:89–100.

21 Sadelain M, Papapetrou EP, Bushman FD. Safe harbours for the integration of new DNA in the human genome. *Nat Rev Cancer* 2012;12:51–58.

22 Mizutani T, Li R, Haga H et al. Transgene integration into the human AAVS1 locus enhances myosin II-dependent contractile force by reducing expression of myosin binding subunit 85. *Biochem Biophys Res Commun* 2015;465:270–274.

23 Ordoval L, Boon R, Pistoni M et al. Efficient recombinase-mediated cassette exchange

in hPSCs to study the hepatocyte lineage reveals AAVS1 locus-mediated transgene inhibition. *Stem Cell Rep* 2015;5:918–931.

24 Bonev B, Cavalli G. Organization and function of the 3D genome. *Nat Rev Genet* 2016;17:661–678.

25 Dekker J, Mirny L. The 3D genome as moderator of chromosomal communication. *Cell* 2016;164:1110–1121.

26 Dixon JR, Selvaraj S, Yue F et al. Topological domains in mammalian genomes identified by analysis of chromatin interactions. *Nature* 2012;485:376–380.

27 Sexton T, Yaffe E, Kenigsberg E et al. Three-dimensional folding and functional organization principles of the *Drosophila* genome. *Cell* 2012;148:458–472.

28 Tang ZH, Luo OJ, Li XW et al. CTCF-mediated human 3D genome architecture reveals chromatin topology for transcription. *Cell* 2015;163:1611–1627.

29 Le Dily F, Bau D, Pohl A et al. Distinct structural transitions of chromatin topological domains correlate with coordinated hormone-induced gene regulation. *Gene Dev* 2014;28:2151–2162.

30 Kimura Y, Oda M, Nakatani T et al. CRISPR/Cas9-mediated reporter knock-in in mouse haploid embryonic stem cells. *Sci Rep* 2015;5:10710.

31 Cong L, Ran FA, Cox D et al. Multiplex genome engineering using CRISPR/Cas systems. *Science* 2013;339:819–823.

32 Mashiko D, Fujihara Y, Satouh Y et al. Generation of mutant mice by pronuclear injection of circular plasmid expressing Cas9 and single guided RNA. *Sci Rep* 2013;3:3355.

33 Okita K, Matsumura Y, Sato Y et al. A more efficient method to generate integration-

free human iPS cells. *Nat Methods* 2011;8:409–U452.

34 Ritz C. Toward a unified approach to dose-response modeling in ecotoxicology. *Environ Toxicol Chem* 2010;29:220–229.

35 Zhou X, Maricque B, Xie MC et al. The human epigenome browser at Washington University. *Nat Methods* 2011;8:989–990.

36 Zhou X, Lowdon RF, Li DF et al. Exploring long-range genome interactions using the WashU Epigenome Browser. *Nat Methods* 2013;10:375–376.

37 Rao SSP, Huntley MH, Durand NC et al. A 3D map of the human genome at kilobase resolution reveals principles of chromatin looping. *Cell* 2014;159:1665–1680.

38 Consortium EP. An integrated encyclopedia of DNA elements in the human genome. *Nature* 2012;489:57–74.

39 Ernst J, Kellis M. ChromHMM: Automating chromatin-state discovery and characterization. *Nat Methods* 2012;9:215–216.

40 Papapetrou EP, Lee G, Malani N et al. Genomic safe harbors permit high beta-globin transgene expression in thalassemia induced pluripotent stem cells. *Nat Biotechnol* 2011;29:73–78.

41 Lombardo A, Cesana D, Genovese P et al. Site-specific integration and tailoring of cassette design for sustainable gene transfer. *Nat Methods* 2011;8:U861–U135.

42 He J, Yang Q, Chang LJ. Dynamic DNA methylation and histone modifications contribute to lentiviral transgene silencing in murine embryonic carcinoma cells. *J Virol* 2005;79:13497–13508.

43 Shorts-Cary L, Xu M, Ertel J et al. Bone morphogenetic protein and retinoic acid-inducible neural specific protein-3 is expressed in gonadotrope cell pituitary adenomas and

induces proliferation, migration, and invasion. *Endocrinology* 2007;148:967–975.

44 Sato J, Kinugasa M, Satomi-Kobayashi S et al. Family with sequence similarity 5, member C (FAM5C) increases leukocyte adhesion molecules in vascular endothelial cells: Implication in vascular inflammation. *PLoS One* 2014;9:e107236.

45 Takahashi Y, Sekine K, Kin T et al. Self-condensation culture enables vascularization of tissue fragments for efficient therapeutic transplantation. *Cell Rep* 2018;23:1620–1629.

46 Takebe T, Sekine K, Kimura M et al. Massive and reproducible production of liver buds entirely from human pluripotent stem cells. *Cell Rep* 2017;21:2661–2670.

47 Takebe T, Enomura M, Yoshizawa E et al. Vascularized and complex organ buds from diverse tissues via mesenchymal cell-driven condensation. *Cell Stem Cell* 2015;16:556–565.

48 Ben-David U, Gan QF, Golan-Lev T et al. Selective elimination of human pluripotent stem cells by an oleate synthesis inhibitor discovered in a high-throughput screen. *Cell Stem Cell* 2013;12:167–179.

49 Bedel A, Beliveau F, Lamrissi-Garcia I et al. Preventing pluripotent cell teratoma in regenerative medicine applied to hematology disorders. *STEM CELLS TRANSLATIONAL MEDICINE* 2017;6:382–393.

50 Itakura G, Kawabata S, Ando M et al. Fail-safe system against potential tumorigenicity after transplantation of iPSC derivatives. *Stem Cell Rep* 2017;8:673–684.

51 Tang C, Lee AS, Volkmer JP et al. An antibody against SSEA-5 glycan on human pluripotent stem cells enables removal of teratoma-forming cells. *Nat Biotechnol* 2011;29:U829–U886.



See www.StemCellsTM.com for supporting information available online.